Multiple synchronization strategies in rhythmic sensorimotor tasks: phase vs period correction

Michael H. Thaut[1,2], **Robert A. Miller**[2], **Leopold M. Schauer**[2]

[1] Department of Music, Colorado State University, Fort Collins, C0 80523, USA
[2] Department of Electrical Engineering, Colorado State University, Fort Collins, C0 80523, USA

Abstract. To characterize synchronisation strategies in the tracking of auditory rhythm with rhythmic finger tapping, the adaptation process after unexpected step changes of an interstimulus interval (ISI) of 500 ms was investigated. Step changes of 2% (10 ms), 4% (20 ms), and 10% (50 ms) of ISI were applied to the stimulus sequence. Synchronisation patterns of 5 subjects were analyzed based on synchronisation error (SE) and interresponse intervals (IRI). A strategy shift contigent upon the size of the introduced step change was detected. After small ISI changes, rapid IRI matching to the new ISI was accompanied by temporarily enlarged SE values, which slowly returned to preferred SE values before the step change. Large ISI changes showed quick SE adaptations accompanied by a temporary overcorrection of IRI. Response asymmetry between ISI decreases and increases emerged, showing a stronger adaptation during ISI increases. A two-dimensional difference equation was formulated to simulate the time series of intertap intervals and explain the control process during IRI and SE adjustments. The system constants were optimized to minimalize the deviations between the computed and the observed response trajectories, consisting of the time series of SE and IRI. It was shown that a successful model fit using a linear two-dimensional difference equation was based on the size and direction of the ISI changes. MANOVA procedures showed that differences in equation parameters during small and large step changes were statistically significant ($P < 0.05$). It is therefore suggested that a uniform model accounting for synchronization responses to all step changes would require the introduction of nonlinear system properties.

1 Introduction

Recent theories explaining the control of rhythmic movement in human motor performance assume the existence of internal timekeepers contributing to the generation and control of repetitive, sequential movements (Ivry and Keele 1989; Kugler and Turvey 1987). These movements may range from repetitive motor acts, as found in gait or finger tapping, to complex patterns with an intricately proportionate timing relationship, as displayed in music or athletic performance (Shaffer 1980). The observation that movement patterns can be executed rhythmically without the presence of external timing cues or feedback (Wing and Kristoffersen 1973) strongly supports the notion of the existence of internal timekeeper systems in the brain. Wing and Kristoffersen (1973) proposed a timekeeper model that delineated two levels of time control: a 'central clock' in the central nervous system responsible for tracking time, and a peripheral source related to the observable movement response in time which reflects the execution process in the motor system. In the model, both control levels are assumed to contribute differentially to the observed variability in the actual timing of movement. However, the time intervals produced by the central clock and the peripheral execution process were also assumed to be mutually independent. In spite of considerable theoretical effort in mathematical modeling and understanding of human movement timing, the neural basis of these systems is not well understood at this point. Timekeeping may actually be achieved by several brain systems jointly contributing to this function in multilevel and/or parallel information processing circuits (Turvey et al. 1989). Different motor tasks may also involve different timekeeper systems.

A special subset in rhythmic motor timing tasks consists of movements synchronized to external rhythms, e.g., auditory, tactile, or visual rhythmic patterns. During execution of these movements internal timekeepers have to be adjusted to track external timing cues. Sensorimotor synchronization underlies and facilitates many tasks of daily living from functional work activities to complex artistic (music, dance) and athletic

Correspondence to: M.H. Thaut
(Fax: 970-491-7541; email: mthaut@lamar.colostate.edu)

performance. Simple synchronization tasks such as the widely studied finger-tapping paradigms to a steady or fluctuating metronome beat are seemingly simple to perform, but the mathematical analysis and models of the actual response patterns are very complex and still raise questions regarding exact synchronization mechanisms and sensorimotor translations.

Mathematical analysis of timing and variability of synchronized finger tapping should reveal two basic types of information: (1) how motor timing is controlled in a series of tapping movements; (2) how internal tap timing is synchronized to the external timekeeper. In general, this information is derived from two directly measurable variables: (1) phase deviations between tap event and stimulus event (SE = synchronization error) and (2) differences between interresponse intervals (IRI) and interstimulus intervals (ISI) (Vorberg and Wing 1996). The goal in a synchronization task is to produce a response sequence with the same actual period as the external stimulus sequence and with a zero phase deviation between the response event and the stimulus event. However, the actual timing of synchronized motor acts fluctuates at each response such that response trains show considerable statistical variability due to various external and internal factors and sources of noise (Gilden et al. 1995; Schulze 1992; Vos and Helsper 1997; Wing and Kristoffersen 1973). The fluctuations in response timing necessitate continuous time adjustments in phase and period durations in order to maintain stable synchronization states. Models of optimal correction strategies have been proposed before, based on differential assessments of the source of the variance in motor timing (Vorberg and Wing 1996). These time adjustments, however, are constrained by the fact that in an ongoing synchronization task, phase and period corrections cannot be accomplished separately and independently. Corrections in one system (e.g., phase

timing) in an unperturbed isochronous tapping task will offset timing in the other system because of the boundary conditions in sequential tapping responses where tap events mark successive tap intervals. This issue can be further demonstrated in ISI sequences with unanticipated step changes in interval duration. After the step change, the original phase relationship can only be restored by temporary overcorrection, i.e., a deliberate timing error in the tapping period (Fig. 1). Likewise, an immediate adjustment of the period will create temporarily a larger phase SE.

The interdependence of phase and period timing has been recognized before. For example, Mates (1994a,b) proposed a detailed timekeeper model specifically for synchronization to an external isochronous rhythmic timekeeper which comprised a period and a phase correction mechanism. The mathematical equations describe in detail all internal and external variables determining the synchronization process and the different sources of noise perturbing the process. However, the equations assume independence between phase and period corrections, expressing the concept that phase relationships between tap and rhythmic signal reflect a positional embeddedness of IRI into the ISI sequence, whereas period corrections refer to serial adjustments, i.e., direct matching and correction of IRI and ISI durations. Hary and Moore (1987) have argued for a motor timing model during steady and systematically varying metronome periods that introduces two alternative phase reset strategies to maintain stability of the interval duration in tapping sequences. The tap event times were determined by adding to the internal reference interval either the previous tap event time or the stimulus event time. However, their model has been critized as not corresponding well to observed data sequences on several issues, e.g., poor SE estimation, small feedback from SE correction, second-order
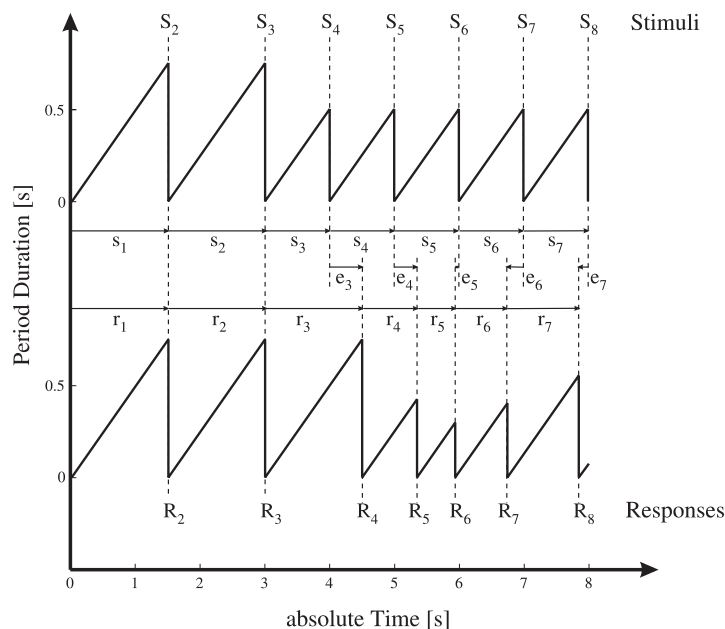
Fig. 1. Relationship between (1) the successive interstimulus intervals (ISI), (2) the controled systems interresponse interval (*IRI*) and (3) the accumulating synchronization error (*SE*). After stimulus 3, ISI s_3 is increased by 20% . IRI r_3 remains unchanged because the system is uncertain about the next ISI s_4. SE e_3 follows logically and influences e_4 together with the next controlled IRI r_4

structure of timekeeper model despite very low correlations beyond lag 1 (Mates 1994a). Vorberg and Wing (1996) have proposed a theoretical model for metronome synchronizations which introduces a phase correction scheme to adjust synchrony between the metronome and IRI period. Although in theory those models exhibit strong robustness to maintain synchronization, empirical verification is not unequivocal. For example, a recent analysis of autocorrelations of synchronization errors and interresponse intervals during finger tapping to a metronome showed different patterns (Thaut and Schauer 1997). Whereas IRI autocorrelations were significantly negative at lag 1, as predicted by Wing and Kristoffersen's model (1973), SE autocorrelations showed positive lag 1 autocorrelations, indicating different adaptation strategies for phase and period corrections. Ivry and Hazeltine (1995) provided data that support interval matching rather than beat stimulus matching as the foundation for synchronization timing based on the observation that temporal variability of tapping intervals was similar under continuous or discontinuous ISI conditions, i.e., feedback from external phase corrections was not necessary to maintain internal rhythmic stability. In using auditory rhythm to entrain gait patterns with Parkinson's disease (PD) patients, we found rapid step synchronization to auditory rhythm, leading to enhanced gait performance (McIntosh et al. 1997; Miller et al. 1996; Thaut et al. 1996). Since aspects of internal timekeeper function are highly compromised in PD due to deficits in basal ganglia function, successful rhythmic entrainment based on sequential phase corrections of a poorly matched or unstable internal clock appears a highly unlikely mechanism.

Therefore, this study sought to clarify further the differential contributions of phase vs period (or frequency = 1/period) locking mechanisms to rhythmic synchronization strategies. For this purpose, we developed an experimental paradigm that, by introducing random step changes in ISI duration into the rhythmic signal sequence, forced the subject to prioritize a choice between phase and period adjustment to maintain rhythmic finger tap synchronization. Furthermore, for mathematical modeling of the response patterns, a set of difference equations was produced to simulate the observed data patterns. The model was also intended to develop mathematical control rules to describe the rhythmic adaptation process, which may help to elucidate control functions of timing mechanisms in future physiological research.

To elucidate phase vs period synchronization strategies further, we investigated two additional questions:

(1) Would a forced choice between phase vs frequency locking be dependent on the size of the step change?
(2) Would a decrease or increase in step changes from the ISI lead to different synchronization adjustments?

2 Subjects and methods

2.1 Subjects

Five right-handed undergraduate students without any known motor, cognitive, or sensory impairment volunteered to participate in the experiment. Their mean age was 22.3 years. The group consisted of 2 male and 3 female participants. The experimental trials were conducted for each subject on 5 separate days spread out over 2 weeks, with each testing session lasting for about 1 h.

2.2 Apparatus

Participants tapped in synchrony with an external rhythmic stimulus using a hand-held 'pencil-shaped' electrode which was tapped on a ground copper plate. The electrode was connected through a 1 megaohm resistor to a 9 volt battery terminal so the timing of a tap event was determined by the change in electrode voltage from 9 volt to ground potential. Software was written (in C+) utilizing a Scientific Solutions A-D Board and LabPac software subroutines to deliver the stimuli and record and analyze the data on an IBM compatible PC. The electrode data were recorded at 1000 samples per second, yielding measurements of SE, IRI, and ISI at a 1 ms resolution. The auditory stimulus was generated with a Grass Audio Click-Tone Module at a frequency of 2 KHz with a 30 ms duration tone burst, 5 cycle rise and fall times, and was delivered to the subject via headphones at a level of 60 dB above the subject's auditory threshold. The occurrence of tap and rhythmic stimuli was measured at the onset of voltage deflection.

2.3 Experimental procedure

Subjects tracked perturbed auditory stimulus sequences at 2 Hz (ISI = 500 ms). A 60 stimulus sequence was delivered beginning with an ISI of 500 ms and changed to a new ISI value randomly chosen between the 25th and 30th event. ISI changes were either 10, 20, or 50 ms. Multiple trials were performed to reduce random variability in IRI which would mask small changes in stimulus rate in the rhythmic sequence. Twenty-five trials of each task were performed for each ISI change. Six trials, one for each of the six interval changes, were presented to the subjects within one block. The presentation order of the six interval changes (+10, −10, +20, −20, +50, −50) was randomized within each block. Each subject performed 25 trial blocks. Rests were given between each block.

2.4 Data analysis

Tapping patterns of every ISI-change trial were averaged for each subject and across subjects. Mean response patterns across subjects were plotted for 10

stimuli prior to and 30 following the step change. Two coupled linear difference equations (see model) were used to create a best fit estimate of the SE and IRI corrections after the step change for each subject and across subjects. The optimal values of the equation constants a and b allowed for a smooth representation of the observed SE and IRI patterns before and after the step change until the SE and IRI values became stationary again. The effect of the step change size on the values of a and b was statistically analyzed using multivariate analysis of variance (MANOVA) procedures.

3 Model of synchronization

The model was based on the following general description of the experiment. A series of equally spaced 'clicks' were provided to the subject as synchronization stimuli over a period long enough to allow the subject to adapt to the stimulus and provide a corresponding series of 'taps' as the synchronization response. A steady-state condition was considered to have been achieved when the taps were in synchrony with the clicks, according to the subject's perception. This steady-state condition provided an initial stationary point for the model to be developed. At a random point in the stimulus sequence, the stimulus interval was changed to a new constant value, and the subjects were given sufficient time to synchronize their responses to the new stimulus interval. The second condition moved the stationary point, and the former system state served as the initial condition of the new relaxation process. The mathematical model was developed to simulate the rhythmic adaptation process adequately during this steady-state shift.

For clarification, the events occurring in absolute time will be indicated by capital letters, and time intervals will be indicated by lower-case letters:

$$R_{n+1} = R_n + r_n \tag{1}$$

$$S_{n+1} = S_n + s_n \tag{2}$$

Here R_n and S_n denote the absolute response times and stimulus times, while r_n and s_n denote the time intervals between two successive response times and stimulus times. The synchronisation error e_n expresses the time interval between the stimulus time S_{n+1} and the corresponding response time R_{n+1}:

$$e_n = R_{n+1} - S_{n+1} \tag{3}$$

As a consequence of this definition, the synchronisation error is positive if the response occurs after the stimulus and negative if it occurs before the stimulus. Also, the first valid synchronisation error (at $n = 1$) occurs after the stimulus interval s_n has been established, i.e., after two stimuli have occurred.

Inserting (1) and (2) into (3) and increasing the index n by 1 results in

$$e_{n+1} = e_n + r_{n+1} - s_{n+1} \tag{4a}$$

To understand the relationship between the controled response interval r_n and the corresponding synchronization error e_n induced by the stimulus interval s_n, refer to Fig. 1. By adding the appropriate time arrows, it follows that

$$e_n + r_{n+1} = s_{n+1} + e_{n+1} \tag{4b}$$

which also follows directly from (4a).

Figure 1 displays the relationships between successive stimuli and the responses of a theoretical controler without any noise. After stimulus S_3, the stimulus interval s_3 is decreased by approximately 33% for better visualization. The response interval r_3 remains unchanged because the controler has no anticipatory information to adapt to the new stimulus interval. After the next stimulus S_4, the theoretical controler can adapt the response interval r_4, based on the last response interval, the synchronization error, and/or the recognized stimulus interval:

$$r_{n+1} = F(r_n, e_n, s_n) \tag{5}$$

The formal expression $F(r_n, e_n, s_n)$ contains all functional dependencies of the immediately following response interval $(n + 1)$ on the current r_n, e_n, and s_n in a mathematical formula and is called the controler function. The time series for r_n and e_n can be calculated by simultaneous application of the coupled difference equations given by (5) and

$$e_{n+1} = e_n - s_{n+1} + F(r_n, e_n, s_n) \tag{6}$$

Equation (6) follows from (4) by inserting (5). Both equations describe a discrete dynamic system with the state variables r_n and e_n and the driving force s_n. The goal of further efforts is to design the controler function to be as simple as possible, while predicting the actual behavior of the biological system.

The first step is the common simplification of the controler $F(\bullet)$ by linearization at a point of the dynamic system which satisfies the stationary conditions. This point, which is characterized analytically by a system state in which the system variables hold constant values, yields the so-called stationarity conditions:

$$r_{n+1} = r_n \tag{7a}$$

$$e_{n+1} = e_n \quad n = 1, 2, 3, \ldots, \infty \tag{7b}$$

This system state can only exist if the driving force s_n is constant long enough for the response to adapt to the constant stimulus intervals indicated by s_{P1}.

$$s_n = s_{P1} \quad \text{for } n > n_R \tag{8}$$

The number n_R denotes the stimulus index indicating the time demand for system relaxation.

To estimate the stationary values of r_n and e_n, the stationarity conditions (7a), (7b), and (8) are inserted into (5) and (6) and solved for the state variables. One obtains the coordinates of the stationary point as

$$r_n = s_{P1} \tag{9a}$$

$$s_{P1} = F(s_{P1}, e_n, s_{P1}) \tag{9b}$$

The stationary response interval is called r_{P1} and is equal to the interstimulus interval s_{P1} according to (9a).

The stationary synchronization error is given implicitely by the solution of (9b) for e_n and is called e_{P1}, so that the following expression is valid:

$$s_{P1} = F(s_{P1}, e_{P1}, s_{P1}) \tag{10}$$

In the state space with the dimensions of response interval r_n and synchronisation error e_n, the stationary point of the system described by (5) and (6) is therefore $\{r_{P1}, e_{P1}\}$. Near this point, we assume the controler to be a linear function of its input variables. This implies the linear dependence of the controler function output on the difference between the initial conditions and the current system state:

$$F() \propto r_n - r_{P1}, e_n - e_{P1}, s_n - s_{P1} \tag{11}$$

The linear approximation is performed by a Taylor series expansion of $F(\bullet)$ about the stationary point, neglecting the terms of order higher than 1:

$$F(r, e, s) = F(s_{P1}, e_{P1}, s_{P1}) + \frac{\partial F}{\partial r} * (r - s_{P1})$$
$$+ \frac{\partial F}{\partial e} * (e - e_{P1}) + \frac{\partial F}{\partial s} * (s - s_{P1}) \tag{12}$$

Incorporating the parameters α, β, and γ for the partial differentials (evaluated at the stationary point) in (12) and applying (10), one obtains as the controler function

$$F(r_n, e_n, s_n) = \alpha * r_n + \beta * e_n + s_{P1} * (1 - \alpha)$$
$$- \beta * e_{P1} + \gamma * (s_n - s_{P1}) \tag{13}$$

If the stimulus interval is changed to the new stimulus interval $s_n = s_{P2}$, the stationary point is shifted. To estimate this shift, (5) and (6) are applied after inserting the specified controler (13) and the stationarity conditions (7a, b). The coordinates of the shifted stationary point are the solution of this proccess:

$$r_n = s_{P2} \tag{14a}$$

$$e_n = e_{P2} \tag{14b}$$

The value of e_{P2} is given implicitly by

$$s_{P2} = F(s_{P2}, e_{P2}, s_{P2}) \tag{15}$$

according to (9b) and using the specified controler (13).

Because the controler $F(\bullet)$ is defined in (13) and has to satisfy this condition, the coordinates of the shifted stationary point $\{s_{P2}, e_{P2}\}$ are substituted into the right side of (15). The resulting equation leads to the description of the relationship between the parameter γ and the final stationary synchronization error e_{P2}:

$$\gamma = 1 - \alpha - \beta * \frac{e_{P2} - e_{P1}}{s_{P2} - s_{P1}} \tag{16}$$

It becomes clear that the value of system parameter γ is determined by the influence of the stimulus intervals before and after changes and the associated stationary synchronisation errors e_{P1} and e_{P2}.

Summarizing (5), (6), (13), and (16), it is noted that the dynamic system is completely described by the pa-

rameters α and β, once e_{P1} and e_{P2} are determined. The equations describe mathematically all possible patterns in the time series of the synchronization errors and response intervals of an oscillator driven by a series of external stimuli, and whose response intervals are linearly dependent on three factors: (1) the preceding interval, (2) two succeeding stimulus intervals, and (3) the synchronization error. The last factor may be interpreted as the phase difference between the pacemaker and the oscillator at the discrete stimulus moments. The values of α and β determine the different temporal behaviors or the synchronisation strategies, respectively, of the system (see Fig. 5). It can be shown that the relaxation behavior of the model with certain system constants α and β fits very well the data of experiments with small and large unexpected steps of ISI. The fit between model data $\{r_n, e_n\}$ and experimental data $\{IRI_n, SE_n\}$ was performed by a steplike optimization process of the model constants α and β. In every step, the model constants were adjusted incrementally, and the maximum value of all the distances was calculated between the points $\{r_n, e_n\}$ and $\{IRI_n, SE_n\}$ of the given experiment. The process was directed to find certain values of the model constants α and β that minimize the differences between both trajectories in state space.

4 Results

4.1 Large ISI changes (± 50 ms)

The averaged responses of IRI and SE to 25 unexpected step changes of 50 ms are shown in Fig. 2. Ten responses before and 30 responses after the period change are plotted. Figure 2a shows how the IRI at tap no. 11 remained at a 500 ms duration since there was no prior knowledge of the rate change and taps in our study sample were anticipatory to the beat. As a consequence of the ISI change, the SE (Fig. 2b) increased to around -50 ms. The response strategy in the next few taps was to increase the IRI, temporarily overshooting the new ISI value (tap no. 12 = about 560 ms; tap no. 13 = 578 ms; tap no. 14 = 570 ms; tap no. 15 = 565 ms, tap no. 16 = 552 ms) in order to return the SE value within approximately 9 taps back to its previous phase relationship. A similar pattern was observable when the ISI was decreased (Fig. 2c, d). There was a slight difference between ISI decrease vs increase. The phase alignment to ISI increases appeared 'stronger', i.e., the SE returned faster to baseline values and even overcorrected before returning toward prestep change values. The broken lines in Fig. 2 mark the computed best fit response pattern based on (5) and (6) in the model, tracking the SE and IRI correction process.

4.2 Small ISI changes

Averaged response patterns of IRI and SE to 25 step changes of 20 ms and 10 ms are shown in Fig. 3 and 4, respectively. The response patterns were markedly different than to large step changes. The new ISI value
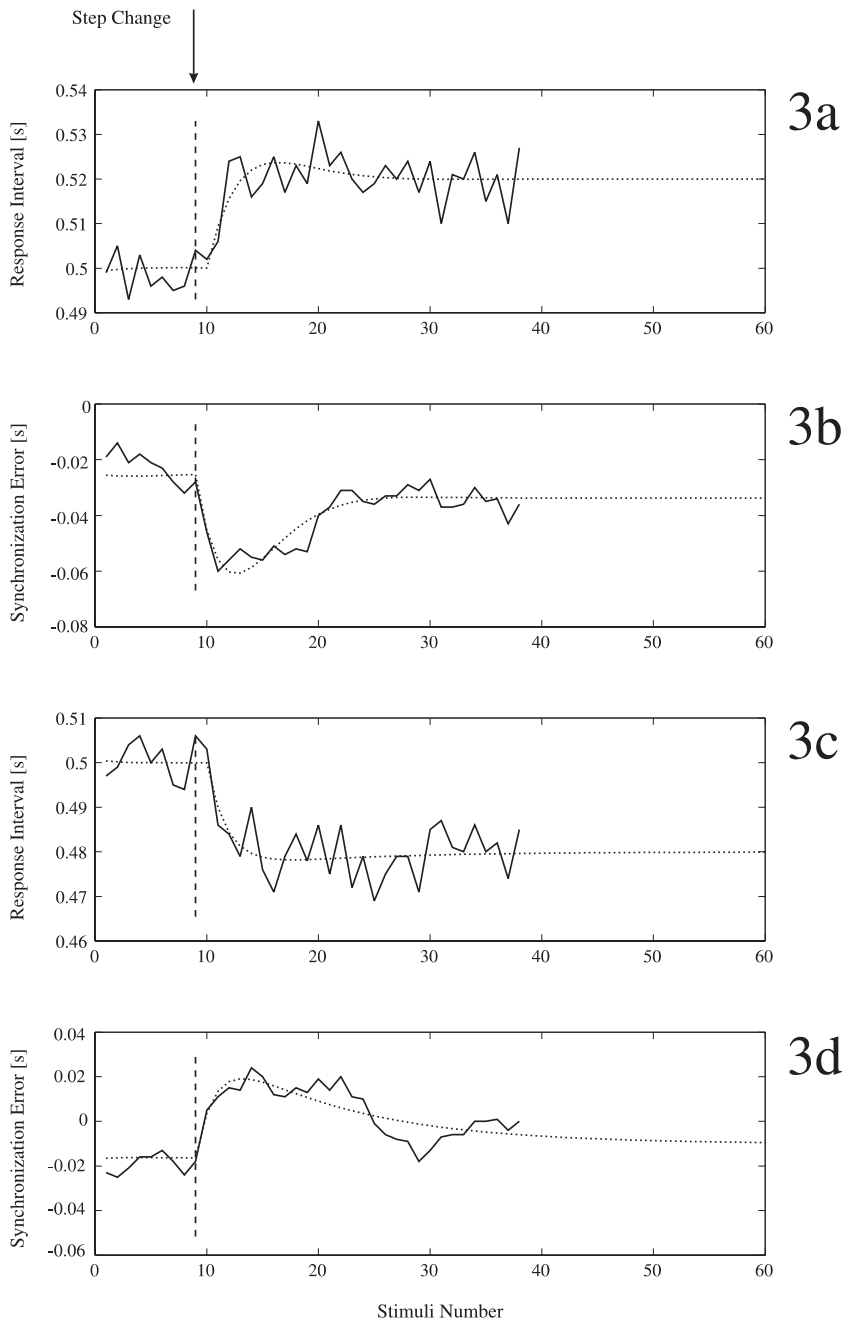
Step Change

2a

2b

2c

2d
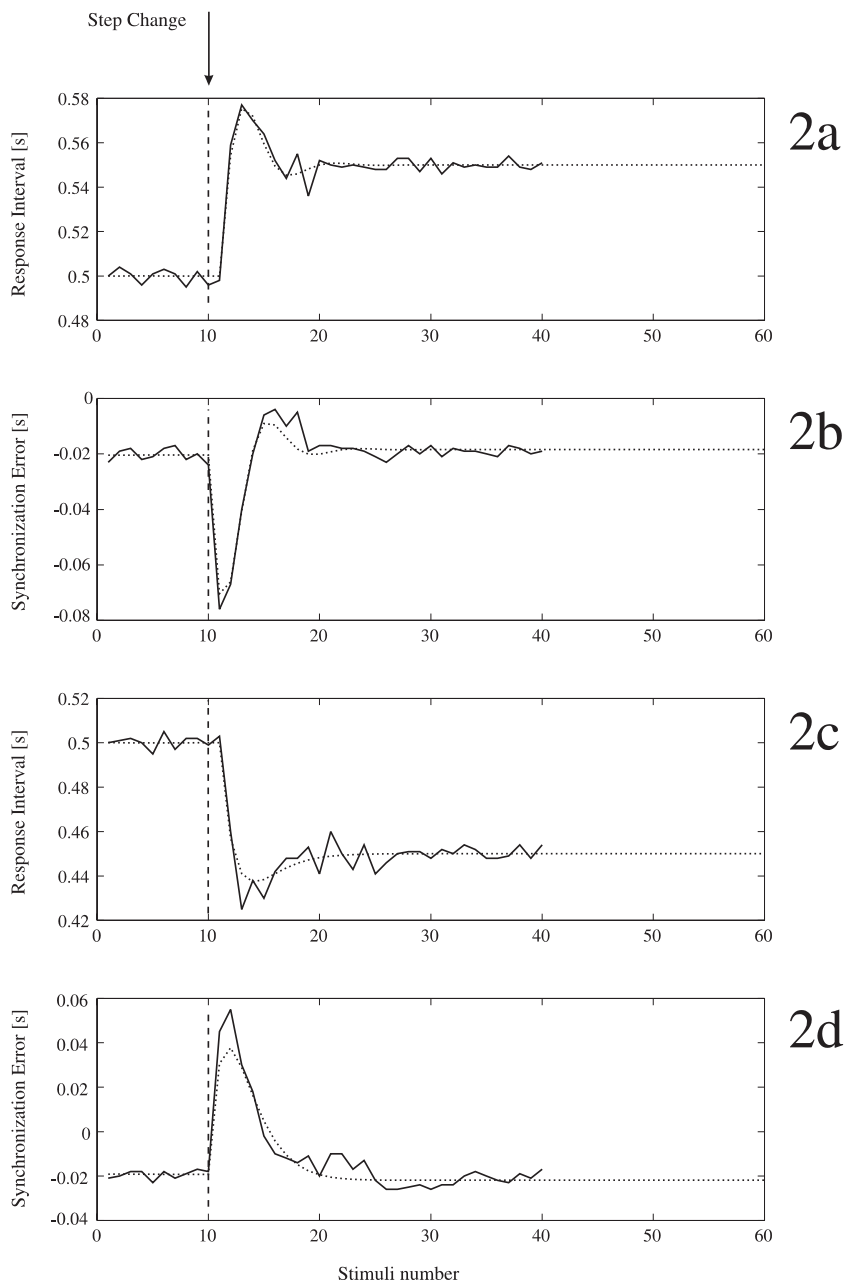
Fig. 2. Mean IRI (**a**) and SE (**b**) responses to ISI increase and ISI decrease (**c** IRI, **d** SE) at 50-ms ISI step changes, indicated by *broken vertical lines*

was matched by an immediate IRI adjustment within approximateley 1–3 taps after the step change without IRI overcorrection. This period adjustment temporarily increased the SE, which returned slowly to baseline values, leading to long time demands for system relaxation, i.e., return to steady state. There was a slight asymmetry between ISI increase and decrease in both the 10 and the 20 ms conditions, where rapid period matching was more evident during ISI increase (frequency decrease), which caused a slower SE recovery than during the ISI decrease (frequency increase).

4.3. Model fit

Table 1 shows the values of the constants α and β of the difference equations (5) and (6) for all step change conditions. In order to assess the model fit, three additional mathematical values were provided by fitting the values of the equation constants to the grand means of IRI and SE across all subjects and trials: (1) the maximal time deviation between the measured and the modeled IRI durations, (2) the Pearson correlation coefficient between the time series of observed IRIs and corresponding simulated response intervals r_i, (3) the Pearson correlation coefficient between the time series of observed SEs and simulated synchronization errors e_i. Correlations were computed across the whole stimulus series 1–40. The high correlation values indicated that approximately 80% of the variability of IRI and SE were explained by our model. The maximal time error between measured and modeled IRI durations was 7 ms, which equaled the noise in the observed data. The values of the system constants showed a clear dependence on

Fig. 3. Mean IRI (**a**) and SE (**b**) responses to ISI increase and ISI decrease (**c** IRI, **d** SE) at 20-ms ISI step changes, indicated by *broken vertical lines*

the size and direction of the ISI step change. In Fig. 5, the values of α and β of the fitted difference equations (5) and (6) are shown averaged for each individual (broken lines) and for the total sample (solid line) across all step changes.

4.4 MANOVA statistics

Statistical analysis of differences in rhythmic adaptation strategies across step change conditions was carried out by comparing the mean values of the model constants fitted to the individual subjects' means of IRI and SE, rather than the actual response data at certain stimulus events. The effect of step size on the size of the system

constants was examined using MANOVA procedures. The results are shown in Table 2. Differences in model constants were insignificant between 10 and 20 ms step changes, suggesting similar synchronization strategies for those two conditions. However, the statistically significant differences between small and large step changes for α and β support the dependence of α and β on the extension of larger ISI changes beyond 2% and 4% of the ISI.

5 Discussion

Two distinct synchronization strategies emerged during ISI step change trials contingent upon the size of the ISI
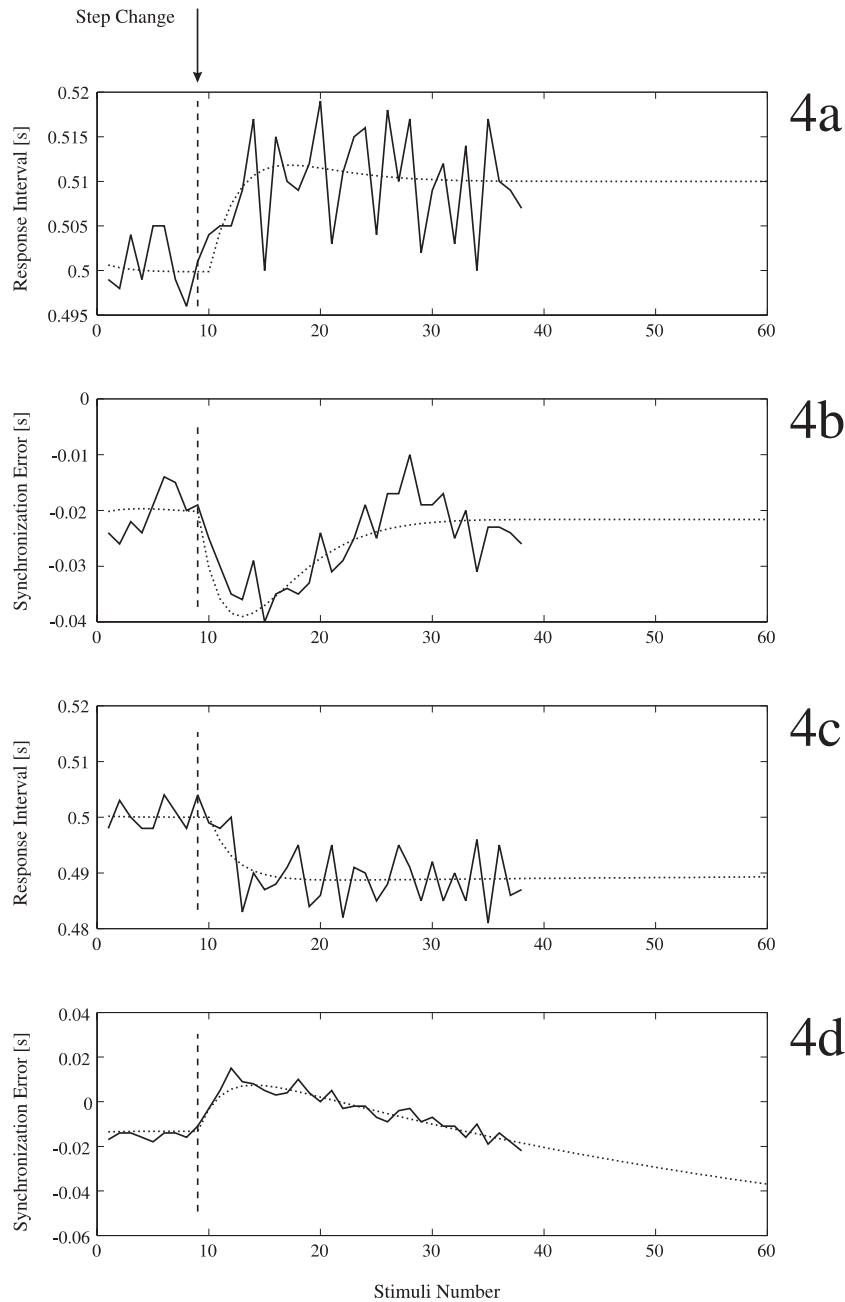
Fig. 4. Mean IRI (**a**) and SE (**b**) responses to ISI increase and ISI decrease (**c** IRI, **d** SE) at 10-ms ISI step changes, indicated by *broken vertical lines*
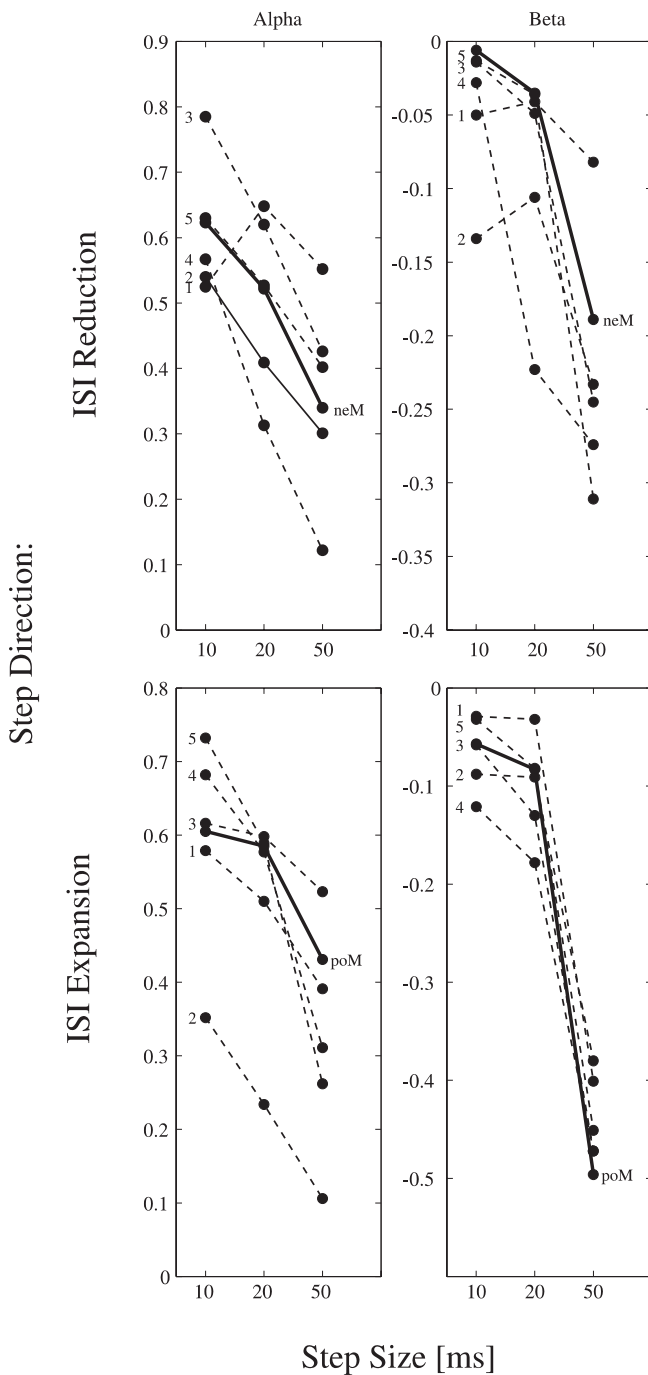
Table 1. Data of model fit: values for α and β, maximal time deviations between measured and modeled IRI durations, correlation coefficients between measured and modeled IRIs and SEs

Step size (ms)	α	β	Deviation (s)	corrIRI	corrSE
+ 10	0.605	−0.057	0.006	0.643	0.763
− 10	0.623	−0.006	0.004	0.784	0.951
+ 20	0.585	−0.083	0.006	0.891	0.909
− 20	0.522	−0.035	0.007	0.879	0.902
+ 50	0.431	−0.496	0.004	0.990	0.973
− 50	0.340	−0.189	0.006	0.981	0.965

change. Larger perturbations (10% of ISI) caused subjects to realign baseline phaselocking of SE and adjust the IRI to the new intervals in similar time scales.

Rapid phase adaptation resulted in a simultaneous temporary timing error in the IRI which needed to be overcorrected to allow for a quick phase correction process. However, rhythmic synchronization during small perturbations (2% and 4% of ISI) was achieved by quickly matching the duration of IRI to the new ISI period and tolerating temporary SE deviations, which recovered gradually to baseline values. The latter strategy suggests that until a certain threshold of change in the ISI is reached, rhythmic synchronization may be primarily driven by duration or period matching and less by a continuous realignment based on the positional time error between the occurrence of the stimulus cue and the tap event, i.e. period locking appears rather than phase locking. Furthermore, an interesting asymmetry in SE and IRI adjustments occurred in our study

Fig. 5. The dependence of the linear system constants α and β on the size and direction of the ISI changes. *Broken lines* display the α- and β-values of the intraindividually averaged responses, and *solid lines* connect the α- and β-values of the averaged responses across all subjects

the time parameter (SE or IRI) that is dominant during response adaptation.

Based on the data in our study and using the descriptive model as a process presentation, one may postulate that during rhythmic synchronization the following task hierarchy emerges: first, a time interval is marked by two stimulus events which generates a precise period template in the brain. The subject embeds this template through finger tapping into the stimulus sequence with a certain phase deviation that is set not to exceed a certain percentage threshold of the target interval (preferred synchronization error). Within this phase error, the subject perceives him/herself to be in synchrony with the rhythmic cue, and synchronization would be primarily driven by direct period matching of IRI to ISI. Only if the phase and period matching error exceeds the threshold setting, phase alignment must temporarily take priority in order to reestablish perceived event-to-action coincidence.

Furthermore, our data indicate that the period matching process after ISI perturbations was accomplished very rapidly and precisely, and that systematic tracking of period errors still took place at a 2% and 4% variation level of the tracking interval. Interestingly, these percentage levels lie below the approximate 5% value of the Weber fraction commonly accepted as the perception threshold for changes in interval durations used in this study (Getty 1975). These values are also below the coefficients of variation of IRI and SE responses (around 5% of the stimulus interval) found in previous synchronization research (e.g., Thaut et al. 1997), which may indicate variance boundaries for normal response fluctuations in synchronization tasks. There may be a difference in the perception of systematic variation (change in ISI interval to a new constant value) vs continuous fluctuations in the IRI response patterns that allow for this precise adjustment to small ISI changes. However, the rapid adaptation to systematic ISI changes after a very small number of repetitions (1 to 3) emphasizes the ability of the auditory system to build very fast temporal templates. Although there is strong support for the existence of cognitive tracking schemes of rhythm in motor performance (Pressing et al. 1996), our data also indicate the ability of rhythmic sensory information in the auditory system to control motor response timing very directly below levels of cognitive awareness, which may imply the existence of purely physiological auditory-motor entrainment mechanisms.

The observed multiple synchronization strategies are expressed in our brief mathematical model through adjustments in the equation constants. Thus, our model accomplishes not only a smooth simulation of the observed response patterns as a pure description but also expresses the functionality of the equation parameters which control the shift in synchronization response. According to our suggested difference equations (5) and (6), a sequential tap interval is computed on the basis of a weighted sum of the preceding tap interval and the preceding synchronisation error. The strategy shift appears in our model as an adjustment of the weights attributed to α and β. At small ISI changes, the small value

between ISI increases and decreases. With large step changes, the SE return to baseline values appeared stronger during ISI increases than decreases. With small step changes where fast IRI matching was prioritized, IRI adjustment appeared quicker in ISI increases than decreases. One may conclude that ISI increases (frequency deceleration) lead to a stronger adaptation process than decreases, and this process is applied to

Table 2. Descriptive and MANOVA statistics for α and β. Each cell contains 10 cases. The cases are counted independently of the direction of ISI change. Diff 1, 2 means the difference between 10 and 20 ms changes, diff 2, 3 means the difference between 20 and 50 ms changes

Step size	α			β		
	(Group mean)	SD	Variance	(Group mean)	SD	Variance
± 10 ms	0.601	0.121	0.015	-0.057	0.044	0.002
± 20 ms	0.503	0.139	0.019	-0.097	0.064	0.004
± 50 ms	0.340	0.150	0.023	-0.332	0.127	0.016
	Probabilities	F-value		Probabilities	F-value	
diff 1, 2	$P = 0.121$	2.561		$P = 0.305$	1.094	
diff 2, 3	$P = 0.013$	7.034		$P = 0.000$	37.669	

of β represents the disregard for adjustments of SE fluctuations to maintain synchrony with a rhythmic stimulus sequence in favor of interval matching. This is true for ISI decreases as well as increases, with the exception of a certain hysteresis shown in Fig. 5. At large ISI changes, the larger corrective influence of phase adjustments is reflected by an expansion of β by a factor of about 10 and a slight reduction in α.

Lastly, our model required a different set of 'calibrations' of the equation constants for different step changes to simulate the empirically observed shift in synchronization strategy. Therefore, rhythmic synchronization strategies may not be expressed sufficiently through linear models. For future research, a self-regulatory model should be designed in which a given set of parameters in a difference equation simulates synchronization responses to step changes of all sizes. However, if these parameters are defined as dependent on the system variables SE and IRI, the ensuing model would have to be one describing a nonlinear system.

The source of noise in the remaining residuals of the fit process and the meaning of the system constant γ reflecting the stationary conditions prior to and after the ISI change could not be investigated here and remain open for further work.

References

Getty D (1975) Discrimination of short temporal intervals: a comparison of two models. Percept Psychophys 18:1–8

Gilden DL, Thornton T, Mallon MW (1995) 1/f noise in human cognition. Science 267:1837–1839

Hary D, Moore GP (1987) Synchronizing human movement with an external clock source. Biol Cybern 56:305–311

Ivry RB, Hazeltine RE (1995) Perception and production of temporal intervals across a range of durations: evidence for a common timing mechanism. J Exp Psychol Hum Percept Perform 21:3–18

Ivry RB, Keele SW (1989) Timing functions of the cerebellum. J Cognit Neurosci 1:136–152

Kugler PN, Turvey MT (1987) Information, natural law, and the self-assembly of rhythmic movement. Erlbaum, Hillside, NJ

Mates J (1994a) A model of synchronisation of motor acts to a stimulus sequence. I. Timing and error corrections. Biol Cybern 70:463–473

Mates J (1994b) A model of synchronisation of motor acts to a stimulus sequence. II. Timing and error corrections. Biol Cybern 70:475–484

McIntosh GC, Brown SH, Rice RR, Thaut MH (1997) Rhythmic auditory-motor facilitation of gait patterns in patients with Parkinson's disease. J Neurol Neurosurg Psychiatry 62:22–26

Miller RA, Thaut MH, McIntosh GC, Rice RR (1996) Components of EMG symmetry and variability in parkinsonian and healthy elderly gait. Electroencephal Clin Neurophysiol 101:1–7

Pressing J, Summers J, Magill J (1996) Cognitive multiplicity in polyrhythmic pattern performance. J Exp Psychol Hum Percep Perform 22:1127–1148

Schulze HH (1992) The error correction model for the tracking of a random metronome: statistical properties and an empirical test. In: Macar F, Pouthas V, Friedman WJ (eds) Time, action, and cognition. Kluwer, Dordrecht

Shaffer LH (1980) Analyzing piano performance: a study on concert pianists. In: Stelmach G, Requin J (eds) Tutorials in motor behavior. North Holland, Amsterdam, pp 443–455

Thaut MH, Schauer LM (1997) Weakly coupled oscillators in rhythmic motor synchronization. Proc Soc Neurosci 298:20

Thaut MH, McIntosh GC, Rice RR, Miller RA, Rathbun J, Brault JM (1996) Rhythmic auditory stimulation in gait training for Parkinson's disease patients. Mov Disord 11:193–200

Thaut MH, Rathbun J, Miller RA (1997) Music vs metronome timekeeper in a rhythmic motor task. Int J Arts Med 5:4–12

Turvey MT, Schmidt RC, Rosenblum LD (1989) 'Clock' and 'motor' components in absolute coordination of rhythmic movement. Neuroscience 33:1–10

Vorberg D, Wing A (1996) Modeling variability and dependence in timing. In: Heuer H, Keele SW (eds) Handbook of perception and action, Vol 2. Motor skills. Academic Press, London

Vos P, Helsper EL (1997) Tracking simple rhythms: on-beat versus off-beat performance. In: Macar F, Pouthas V, Friedman WJ (eds) Time, action, and cognition. Kluwer, Dordrecht

Wing AM, Kristoffersen AB (1973) The timing of interresponse intervals. Percept Psychophys 13:455–460